Alterations in plasma membrane promote overexpression and increase of sodium influx through epithelial sodium channel in hypertensive platelets

D. Cerecedo [a,*], Ivette Martínez-Vieyra [a], Alejandro Sosa-Peinado [b], Jorge Cornejo-Garrido [c], Cynthia Ordaz-Pichardo [c], Claudia Benítez-Cardoza [d]

[a] Laboratorio de Hematobiología, Escuela Nacional de Medicina y Homeopatía (ENMH), Instituto Politécnico Nacional (IPN), México City, México
[b] Departamento de Bioquímica, Facultad de Medicina, Universidad Nacional Autónoma de México (UNAM), P.O. Box 70-159, 04510, D.F., México City, México
[c] Laboratorio de Biología Celular y Productos Naturales, ENMH, IPN, México City, México
[d] Laboratorio de Bioquímica, ENMH, IPN, México City, México

ARTICLE INFO

ABSTRACT

Platelets are small, anucleated cell fragments that activate in response to a wide variety of stimuli, triggering a complex series of intracellular pathways leading to a hemostatic thrombus formation at vascular injury sites. However, in essential hypertension, platelet activation contributes to causing myocardial infarction and ischemic stroke. Reported abnormalities in platelet functions, such as platelet hyperactivity and hyperaggregability to several agonists, contribute to the pathogenesis and complications of thrombotic events associated with hypertension.

Platelet membrane lipid composition and fluidity are determining for protein site accessibility, structural arrangement of platelet surface, and response to appropriate stimuli. The present study aimed to demonstrate whether structural and biochemical abnormalities in lipid membrane composition and fluidity characteristic of platelets from hypertensive patients influence the expression of the Epithelial Sodium Channel (ENaC), fundamental for sodium influx during collagen activation. Wb, cytometry and quantitative Reverse Transcription-Polymerase Chain Reaction (qRT-PCR) assays demonstrated ENaC overexpression in platelets from hypertensive subjects and in relation to control subjects. Additionally, our results strongly suggest a key role of β-dystroglycan as a scaffold for the organization of ENaC and associated proteins.

Understanding of the mechanisms of platelet alterations in hypertension should provide valuable information for the pathophysiology of hypertension.

© 2016 Elsevier B.V. All rights reserved.

1. Introduction

Platelets play a critical role in maintaining hemostasis, which is accomplished by platelet aggregation, forming a clot at the site of injury to a blood vessel. Upon contacting the damaged vessel wall, platelets rapidly slow down and adhere to the exposed subendothelial ExtraCellular Matrix (ECM), which contains thrombogenic macromolecules responsible for firm adhesions and cell activation.

Activated platelets undergo reorganization of their cytoskeletons, which translates into shape changes and the release of their intracellular granule contents, strengthening the activated state of the cells to recruit additional platelets to the injury site. This results in the formation of a hemostatic thrombus to seal the wounded vessel [1]; aberrant thrombus formation has severe pathological consequences, leading to fatal thromboembolism and tissue ischemia of vital organs.

Hypertension is a common illness that affects >972 million persons in the world and accounts for 9.4 million deaths each year [2], 45% of deaths due to heart disease and 51% to stroke as a consequence of activated platelets [3]. The latter in turn release vasoactive agents and growth factors contributing to cardiovascular complications associated with hypertension [4,5]. In response to hypertension, platelets display different morphological [6] and biochemical modifications, including altered Ca^{2+} metabolism [7], increased production of Reactive Oxygen Species (ROS), and altered Nitric Oxide (NO) bioavailability [8].

These biochemical modifications could involve mechanisms related with alterations of membrane fluidity and microviscosity that might also affect membrane permeability, transport systems, receptor functions, or enzyme activities. Additionally, it has been suggested that membrane fluidity can be modified by the state of membrane components, the cytoskeletal proteins, and the intracellular Ca^{2+} and sodium Na^+ contents [9].

* Corresponding author at: Laboratorio de Hematobiología, Escuela Nacional de Medicina y Homeopatía (ENHM), IPN, Guillermo Massieu Helguera No. 239, Col. La Escalera Ticomán, 07320 CDMX, México.
E-mail address: dcereced@prodigy.net.mx (D. Cerecedo).

The Epithelial Sodium Channel (ENaC) a highly selective Na^+ channel is involved in mechanosensation, nociception, fluid volume homeostasis, and control of arterial blood pressure [10,11]. In platelets, ENaC is dispensable for migration and alpha and dense granule secretion, whereas Na^+ influx through this channel is fundamental for platelet collagen activation and in addition, it is associated with intermediate filaments and proteins from the Dystrophyn–Glycoprotein Complex (DGC) [12].

The DGC is a multimeric transmembrane protein complex in which Dystroglycan (Dg) is the central protein [13]. Dystroglycan is composed of α and β subunits that are non-covalently associated [14]. The α subunit of Dystroglycan (α-Dg) is an extracellular protein that binds laminin and laminin G-like domains of other ligands [15,16,17]; while the β subunit of Dg (β-Dg) has a single transmembrane domain, and its cytoplasmic tail binds dystrophin [18]. In this manner, Dg forms a transmembrane link between the ECM and the actin cytoskeleton through its interactions with laminin and dystrophin. The cytoplasmic domain of β-Dg is associated with the Ras/MAPK signalling pathway through the adapter protein Grb2 [19]. This evidence reveals that β-dystroglycan plays a dual role: as a mechanical adhesion and as a signalling molecule.

Because the composition and properties of the plasma membrane influence the functions of proteins embedded in membranes, the aim of the present study was to investigate whether there was a structural abnormality or alterations in the composition of the plasma membrane related with ENaC expression and sodium influx in platelets from hypertensive patients. Therefore, we determined protein expression by Western blot and Flow Cytometry (FC) assays and, by qRT-PCR, the messenger RNA (mRNA) expression of ENaC. Additionally, we evaluated membrane characteristics such as platelet membrane fluidity, platelet membrane cholesterol, phosphatidylserine, phosphatidylcholine, and sphingosine, as well as caveolin-1 and β-dystroglycan expression as integral membrane proteins. Correlation of the alterations found in plasma and in the platelet biochemical profile with arterial tension was discussed.

2. Experimental section

2.1. Materials

The populations studied included 25 controls and 25 patients with essential hypertension who gave signed consent for the procedure to be carried out. Anthropometric data and relevant characteristics of the two groups are presented in Table 1. Individuals were defined as hypertensive if, on three consecutive occasions, Systolic Blood Pressure (SBP) was >140 mmHg or if the Diastolic Blood Pressure (DBP) was >90 mmHg. The subjects were following their usual diets, which appeared to be comparable, on the basis of informal dietary histories; all patients were already diagnosed and were receiving

Table 1
General characteristics of hypertensive patients and controls.

Parameter	Hypertensive	Controls
Sex (%male/%female)	21/79	45/55
Age ± SD (years)	61 ± 8.9	39 ± 10
BMI	28.6 ± 3.09	23 ± 2.16
Platelet count × 10^3 (μl)	246.5 ± 144	234.1 ± 130.3
SBP (mmHg)	131 ± 18	116 ± 6
DBP (mmHg)	84 ± 13	77 ± 10
Glucose mg/dl	93.1 ± 6.6	92.7 ± 6.7
Total Cholesterol mg/dl	94 ± 18.8	101 ± 41
Tryglycerids mg/dl	74 ± 14.8	49.5 ± 20
Cortisol (pg/ml)	7305 ± 5298	7021 ± 4671
Aldosterone (pg/ml)	54.65 ± 19.79	18.32 ± 19.8

Values are the mean ± SD of 25 patients and controls in each group.
BMI, body mass index; SBP, systolic blood pressure; DBP, dystolic blood pressure.

treatment. Patients with diabetes mellitus and dyslipidemias were not included in the study.

2.2. Platelet isolation

Platelets were obtained by venopuncture from healthy controls who had not received any drug during the 10 days prior to sampling and from hypertensive subjects under treatment; both populations signed informed consent for the procedure to be carried out. Blood was immediately mixed with citrate anticoagulant including dextrose at pH 6.5 (93 mM sodium citrate, 70 mM citric acid, and 140 mM dextrose) at a blood:anticoagulant ratio of 9:1. Platelet-rich plasma was obtained from total blood by centrifugation at 100 ×g for 20 min at room temperature and was subsequently mixed with an equal volume of citrate anticoagulant and centrifuged at 400 ×g for 10 min. The platelet pack was suspended and washed twice with Hank's Balanced Saline Solution (HBSS) without calcium (137 mM NaCl, 5.3 mM KCl, 1 mM $MgCl_2$, 0.28 mM $Na_2HPO_4.12H_2O$, 0.87 mM NaH_2PO_4, 0.44 mM KH_2PO_4, 4.1 mM $NaHCO_3$, and 5.5 mM glucose).

2.3. Chemicals and standards

High-Performance Liquid Chromatography (HPLC)-grade solvents, chloroform (CHCl3), and Methanol (MeOH) HPLC grade, were obtained from J.T. Baker (Center Valley, PA, USA), while standard phospholipids of biological origin, cholesterol, PG from chicken egg, PhosphatidylCholine (PC) from egg yolk, PhosphatidylSerine (PS) from bovine brain, and SphingoMyelin (SM) from bovine brain were purchased from (Sigma-Aldrich, St. Louis, MO, USA).

2.4. Analysis of cell-surface antigens by immunofluorescence flow cytometry

Platelets from hypertensive and control individuals were incubated with monoclonal antibody for 30 min at 4 °C, washed twice with Phosphate-Buffered Saline (PBS) solution, and suspended for 30 min at 4 °C in with the corresponding secondary antibody (Molecular Probes Kallestad Laboratories, Inc., Austin, TX, USA). Then, the cells were washed three times and subjected to immunofluorescence flow cytometry in a FACScan (Becton Dickinson, San Jose, CA, USA). Fluorescence data were collected in log scale. Results were indicated as percentages of positive cells for each antigen.

2.5. Aldosterone and cortisol determination

Blood serum from controls and hypertensive patients were processed by Enzyme-Linked Immunosorbent Assay (ELISA) for quantitative detection of aldosterone and cortisol levels (Enzo Life Sciences, Inc., Ann Arbor, MI, USA) according to the manufacturer's instructions. Plates were read at 405 nm on a microplate reader (Molecular Devices, Sunnyvale, CA, USA) using soft-max-Pro software (Molecular Devices). A standard curve was plotted, and the aldosterone and cortisol concentration in each sample was determined by interpolation from the standard curve.

2.6. Antibodies used

Epithelial sodium channel alpha rabbit polyclonal antibody (Cat. No. ab65710) was purchased from (Abcam, Cambridge, MA, USA) and mouse anti-β-dystroglycan (MANDAG2), from the Developmental Studies Hybridoma Bank. Caveolin-1 polyclonal antibody (Cat. No. sc-53564) and p-Thr mouse monoclonal antibody (H-2) were obtained from Santa Cruz Biotechnology, Inc. (Santa Cruz, CA, USA) and β-dystroglycan polyclonal antibody PY892 (Cat. No. 617102) was purchased from (Biolegend, San Diego, CA, USA).

2.7. Western blotting

Lysates from 1×10^6 resting and adherent platelets obtained in Sodium Dodecyl Sulfate (SDS) and β-mercaptoethanol were boiled for 5 min, subjected to 10% SDS-PolyAcrylamide Gel Electrophoresis (PAGE), and transferred onto nitrocellulose membranes using a semi-dry system (Thermo Electron Co., Milford, MA, USA). Membranes were incubated with appropriate primary antibodies, then with HorseRadish Peroxidase (HRP)-conjugated secondary antibodies visualized using an enhanced chemiluminescence Western blotting analysis system (Santa Cruz Biotechnology, Inc.) and were subsequently documented using T-mat G/RA film (Kodak, Rochester, NY, USA). Negative controls comprised transferred strips incubated solely with HorseRadish Peroxidase (HRP)-conjugated secondary antibodies. Densitometry analysis was performed by Win Image Studio Digits Ver 4.0 (LI-COR, Inc., NE, USA) software using GAPDH as a loading control to normalize the data.

2.8. Immunofluorescence staining

Meg-01 cells were adhered with poly-D-lysine-coated coverslips and, after 60 min, were permeabilized and fixed with a mixture of 2% p-formaldehyde, 0.04% NP40 in the cytoskeleton stabilizing solution PHEM??? and triton 0.2%. Meg-01 cells were first incubated with the specific primary antibody diluted in PBS 0.1% Bovine Serum Albumin (BSA) to b-Dg MANDAG2 (Pereboev, A., 2001) and incubated for 2 h. Cells were washed with PBS solution and incubated for 1 h with secondary anti-goat, anti-mouse conjugated to Alexa-Fluor-568 (Molecular Probes, Eugene, OR, USA). For counterstaining, nuclei were dyed for 30 min with 40,6-diami-dino-2-phenylindole (Sigma Chemical Co.), washed, and mounted. Slides were observed using a Leica confocal instrument model TCS-SP5 Mo, and images were taken at $63\times$ zoom $3\times$ at 1024×1024 pixels with an HCX PL APO 63/1.40–0.60 DIL CS oil immersion. Optical sections [z] were captured at 0.18 mm. Immunofluorescence quantification was performed using ImageJ (NIH, Bethesda, MD, USA) from 25 cells observed from 3 independent experiments.

2.9. Electron microscopy

Suspended platelets were fixed in 2.5% glutaraldehyde/formaldehyde in Dulbecco's Phosphate-Buffered Saline (DPBS) solution with a pH of 7.4 for 30 min. Platelets were rinsed in phosphate buffer for 5 min before being fixed for 30 min with 1% Osmium tetraoxide (OsO4). The samples were then rinsed 3 times with PBS for 5 min and were dehydrated serially in 30, 50, 70, and 90% and three times in 100% ethanol. The material was critical point dried, mounted, and coated with carbon. Samples were observed with a Jeol Scanning Microscope JSM-6510, and micrographs were taken at 25 kV. The representative platelet area from hypertensive patients and controls was measured using ImageJ software (U.S. National Institutes of Health [NIH], Bethesda, MD, USA).

2.10. Fluorescence measurements

TMA-DPH at a final concentration of 1 mM was incubated at room temperature with a suspension of 2×10^7 washed platelets/ml in a solution of sodium/potassium–Tris medium (137 mM NaCl, 5.4 mM KCl, 11 mM dextrose and 25 mM Tris–HCl adjusted to ph7.4 for 20 min, after which the platelets were centrifuged and resuspended in the same solution. The final concentration of the solvent *N,N*-dimethylformamide was maintained at <0.02 vol%. All fluorescence measurements were performed in quartz cuvettes and were recorded at 25 °C under moderate stirring (250 rpm) with an ISS PC1 Photon Counting Steady-state Spectrofluorometer (Champaign, IL, USA), coupled with Vinci software. Excitation and emission wavelengths were set at 365 and 428 nm, respectively. Fluorescence anisotropy and polarization were automatically calculated for the software.

2.11. RNA isolation

RNA was isolated from control and hypertensive platelets utilizing TRIzol® LS Reagent (Ambion, Life Technologies Corp., Carlsbad, CA, USA) and dissolved in 25 μl of ultrapure water. The quantity of RNA was measured using a spectrophotometer (NanoDrop 2000c; Thermo Scientific, Inc). Samples with RNA concentration (A260/A280 ≥ 1.8 ng/μl) and purity (A230/A260 ≥ 2.0 ng/μl) were selected.

2.12. Quantitative reverse transcription-PCR (qRT-PCR)

qRT-PCR was performed employing the KAPA SYBR FAST One Step qRT-PCR kit (Kapa Biosystems, Inc., Wilmington, MA, USA). Primers were α-ENaC forward (5′CTTTGGCATGATGTACTGGCA-3′) and reverse (5′-GGAAGACGAGCTTGTCCGAGT-3′) [20] and GAPDH. PCR were performed in a 20-μl total reaction volume in a Step One Real Time PCR system (Applied Biosystems, Foster City, CA, USA. An initial cycle step at 95 °C for 5 min was followed by 40 cycles with a 12-s denaturation at 95 °C, 12 s annealing with a temperature of 64 °C, followed by a 12-s primer extension at 72 °C, and finally, for 15 s at 95 °C to ensure complete extension, and for 1 min at 60 °C and 15 s at 95 °C to generate a melt curve. PCR products were visualized by means of 1.0% (*w/v*) agarose gel containing ethidium bromide. The comparative CT (ΔΔCT) method was selected to determine the amount of target nucleic acid sequence in each sample relative to that of the control samples.

2.13. Sodium influx

[Na+]i was evaluated in platelets suspended in 140 mM NaCl, 4.9 mM KCl, 1.2 mM MgCl$_2$, 1.4 mM KH2PO$_4$, 5.5 mM glucose, and 20 mM HEPES (pH 7.4) Platelets were loaded with the SBFI sodium-sensitive fluorescent dye (10 μM) (Life Technologies, Eugene, OR, USA), as we have described previously [12]. The time course was recorded of the fluorescence emission of platelet cells upon collagen activation (10 μg/ml), and each sample was recorded using an LS-55 Spectrofluorometer (Perkin-Elmer, Waltham, MA, USA) equipped with a water-jacketed cell holder for temperature control. All experiments were performed using cells with a 0.4-cm path length at 25 °C. Excitation wavelengths were either 345 or 385 nm, correspondingly, and the fluorescence emission was collected at 500 nm.

2.14. Platelet membrane lipids

Platelets (2×10^6) from hypertensive and control individuals were lysed with 100 μl of a 2× lysis buffer (0.5% NP-40, 2 mM Na$_3$VO$_4$, PSMF) containing a protease inhibitor cocktail and diluted to 1000 μl with PBS solution containing 1 mM of resveratrol (Sigma-Aldrich Co., St Louis, MO, USA). This suspension was extracted with 3 ml of chloroform:methanol (2:1, v:v) by stirring with a vortex for 2 min. The mixture was centrifuged for 5 min at 2000×*g*. Chloroform fraction was obtained and evaporated to dryness under reduced pressure at room temperature in a BÜCHI R-215 Rotary Evaporator, coupled with a BÜCHI V-700 Vacuum Pump and a cold-water recirculating BÜCHI Chiller F-105 (BÜCHI Labortechnik AG, Flawil, Switzerland). The extract recovered was diluted in 1 ml of methanol for its analysis.

2.15. Platelet membrane lipid quantification

High Performance Liquid Chromatography (HPLC) was carried out with an Agilent 1220 Infinity LC System Controller attached to an UltraViolet (UV) light detector, which was programmed to process data at 205 nm at 0.013-min (40-Hz) resolution. Control of equipment, data acquisition, processing, and handling of chromatographic information were accomplished by the EZChrom Elite Compact software program (Agilent). Analyses were undertaken on a Zorbax RX-C18

column (4.6 × 250 mm, 5-μm particle sizes, Agilent) coupled with a Zorbax RX-C18 guard column (4.6 × 12.5 mm, 5-μm particle sizes, Agilent). An isocratic mobile-phase methanol:acetonitrile (80:20) system was employed (HPLC grade; J.T. Baker, Ecatepec, Edo. Méx., México). The flow rate was maintained constant at 1.0 ml/min for 30 min. All standards and samples were solubilized in methanol (1 ml), and a volume of 20 μl was injected. A standard curve of four lipid mixtures was performed, injecting serial dilutions from $2.5 \times 10{-2}$ to $2.5 \times 10{-3}$ mg/ml (Cholesterol) or from 2.5×10^{-1} to 2.5×10^{-2} mg/ml for D-Sphingosine, 1,2-Diacyl-*sn*-glycero-3-phospho-L-serine, and L-α-Phosphatidylcholine (Sigma-Aldrich, St. Louis MO, USA). The peak area obtained for each of the samples was extrapolated from the standard curve, thereby obtaining the lipid concentration in each of the extracts. The results are reported as μg of lipid (standard) content per mg of protein. We included sphingosine, which forms a primary part of sphingolipids, a class of cell membrane lipids that includes sphingomyelin, an important and abundant phospholipid.

2.16. Meg-01 cell culture and differentiation

Meg-01 cells were cultured in RPMI-1640 medium supplemented with 10% Fetal Bovine Serum (FBS), 400 mM L-glutamine, 50 lM gentamicin, 25 mM HEPES, 2 g/l sodium bicarbonate, and 1 mM sodium pyruvate in a humid atmosphere of 5% CO_2 at 37 °C. For differentiation into a megakaryocyte phenotype, Meg-01 cells (diffMeg) were differentiated with I 2–0-TetradecanoylPhorbol-I 3-Acetate (TPA) 10^{-7} M for 7 days [21]. Cell viability was assessed by exclusion of 0.2% Trypan blue and was routinely >90% before and after differentiation.

2.17. Plasmids and transfection

Short hairpin RNA (shRNA) constructs targeting dystroglycan or control shRNA were purchased from GeneCapoeia, Rockville, MA, USA) (ID: HSH003950-CH1). Meg-01 cells (2×10^6/ml) were transfected with 2 μg psi-H1 using a Nucleofector II (Amaxa), according to the manufacturer's recommendation (Lonza Walkersville, Inc., Walkersville, MD, USA). Twenty-four hours later, transfection cells were selected. For functional assays, selected cells were differentiated for 7 days.

2.18. Statistical analysis

Statistical analysis was carried out with the GraphPad Prism® for Windows ver. 5 software (GraphPad Software, Inc., La Jolla, CA, USA). Relative protein expression and relative mRNA expression were analyzed with an unpaired Student *t* test. Statistical significance was defined as *p* < 0.05.

3. Results

The present study included 25 patients and controls of both genders. Table 1 presents a summary of the sociodemographic characteristics of the sample. For BMI, categories were considered as follows: Underweight ≤ 18.5; Normal weight = 18.5–24.9; Overweight = 25–29.9, and Obesity = 30 or over.

3.1. ENaC Is overexpressed in HTA platelets

Recently, by means of an RT-PCR strategy and Western blot-based detection, we reported the expression of ENaC in platelets from healthy individuals [12].

Total platelet lysates of normal individuals and of hypertensive patients were processed for Western blot assays using and anti-α-ENaC polyclonal antibody. The α-ENaC antibody detected the corresponding band migrating to ~75 kDa; GAPDH was employed as load control (Fig. 1A). We quantified the relative expression level of α-ENaC by Western blotting, and our results demonstrated significant overexpression of the channel in hypertensive patients compared with healthy subjects (Fig. 1B). To further confirm these results, platelets from hypertensive patients were processed for immunofluorescence flow cytometry analysis. Mean Fluorescence Intensity (MFI) for hypertensive patients corresponded to 12.76 ± 3.373, while controls had 6.521 ± 2.506.

Finally, to confirm increased protein expression, we performed α-ENaC mRNA relative expression by qRT-PCR assays (Fig. 1C). Our results indicate that the mRNA and the protein corresponding to α-ENaC were more expressed in hypertensive compared with normal subjects.

3.2. Altered influx of ENaC in hypertensive platelets

To corroborate the functionality of ENaC in hypertension, 10 μg/ml of collagen was added to activate platelets from control and hypertensive subjects to measure $[Na]_I$ (sodium influx). Both samples were excited at 345 and 385 nm, and the ratio of fluorescence-emission intensities was registered at 500 nm, as previously described [12]. Fig. 2A depicts the representative plots displayed for control samples with baseline values of 2.0 fluorescence units of $[Na]_I$; collagen added increased $[Na]_I$, with registered values of up to 2.2, reaching baseline values after 100 s. The behavior is noteworthy of the samples of some controls and patients. There were few control samples in which response to collagen corresponded to an inverted slope prior to reaching baseline values.

In general, the $[Na]_I$ in the patients' samples increased from baseline values up to 2.35, which were maintained for >300 s, compared with controls; however, some heterogeneous behaviors were observed. Patients 4 and 10 (Fig. 2B) and patient 6 (Fig. 2C) exhibited $[Na]_I$ values that dropped to 1.4 or to 1.6 (Fig. 2D), respectively, without any increase in $[Na]_I$ values. Fig. 2C presents the $[Na]_I$ of 4 patients and 1 control, who belonged to the same family and who showed different sodium influx; patient 19 did not register $[Na]_I$, in contrast to control 10 who sustained $[Na]_I$ and did not reach baseline values. Fluorescence values of $[Na]_I$ of patients with non-controlled arterial tension plotted in Fig. 2D were heterogeneous and did not reflect arterial tension values.

Our results clearly suggest the presence of abnormalities in $[Na]_I$ in hypertensive patients, owing to ENaC properties.

3.3. Caveolin is overexpressed in hypertensive platelets

Membrane microviscosity is one of the physical properties of cell membrane that modified in hypertension [9]. To assess feasible abnormalities in platelet membrane, we measured the fluorescence polarization of TriMethylAmmonium-DePhenylHexatriene (TMA-DPH) incorporated into the lipid bilayer of suspended platelets from hypertensive and normotensive subjects. Fluorescence anisotropy of TMA-DPH was significantly decreased in platelets of hypertensive patients compared with those of control subjects (Fig. 3A), while polarization values increased and were expressed as membrane microviscosity (1/P) (Fig. 3B). These results clearly indicate that hypertension was associated with an increase of membrane fluidity.

To investigate whether the increase of plasma-membrane fluidity in hypertensive platelets exerted an effect on caveolin-1 expression, we performed Wb of platelet lysates from hypertensive and control subjects using an antibody directed against caveolin-1. Bands corresponding to caveolin-1 were more expressed in platelets from hypertensive patients compared with the bands of non-hypertensive subjects; normalization of caveolin-1 relative values with GAPDH demonstrated significant differences (Fig. 3C).

To ascertain that differences in membrane microviscosity were evident, suspended and collagen-activated platelets from hypertensive and normotensive individuals were processed by scanning electron microscopy. Fig. 3D presents representative images of control and
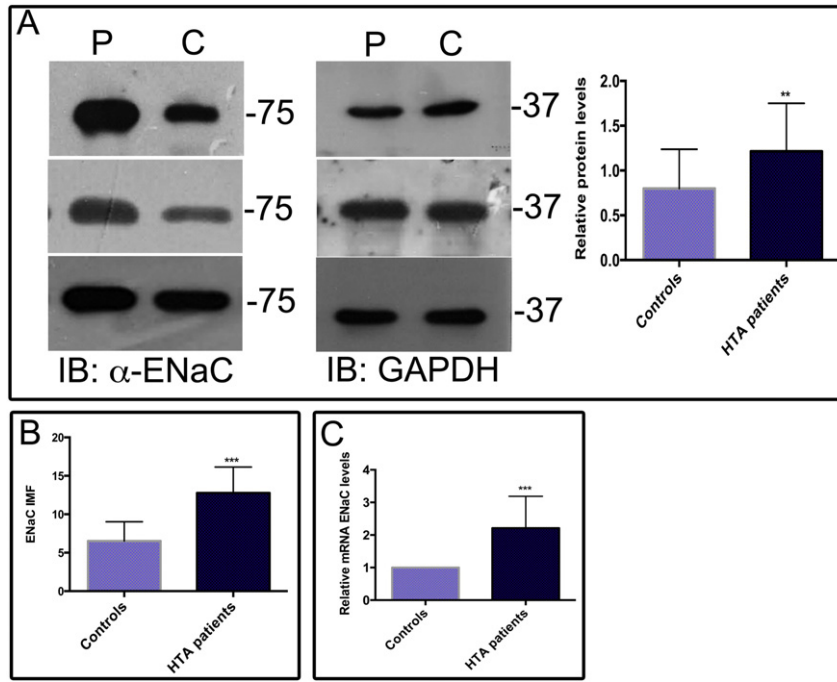
Fig. 1. Epithelial Sodium Channel (ENaC) is overexpressed in hypertensive patients A. Total lysates of hypertensive and control individuals were analyzed by Western blot utilizing antibodies against α-ENaC (75 kDa). Quantitative analysis using GAPDH as loading control depicted. B) Values shown are mean ± Standard Deviations (SD) from bands of the 24 patients with Arterial HyperTension (AHT) and controls. **$P < 0.005$. B. Mean Fluorescence Intensity (MFI) of α-ENaC was quantified by Flow Cytometry (FC) from hypertensive and control individuals. Values shown are mean ± Standard Deviations (SD) from the 24 patients with Arterial HyperTension (AHT) and controls. ***$P < 0.005$. C. Messenger RNA (mRNA) expression of α-ENaC was examined by quantitative Reverse Transcription-Polymerase Chain Reaction (qRT-PCR) of hypertensive and control individuals. Values presented are mean ± Standard Deviations (SD) from the 24 patients with Arterial HyperTension (AHT) and controls. ***$P < 0.05$.

hypertensive platelets; resting control platelets were characterized by the presence of short filopodia, which were numerous and with discrete pores in collagen-activated platelets. Resting and collagen-activated platelets from hypertensive patients showed extensive filopodia protrusion and presence of microvesicles, even under resting conditions (arrows) (Fig. 3D). Although these morphological changes could not
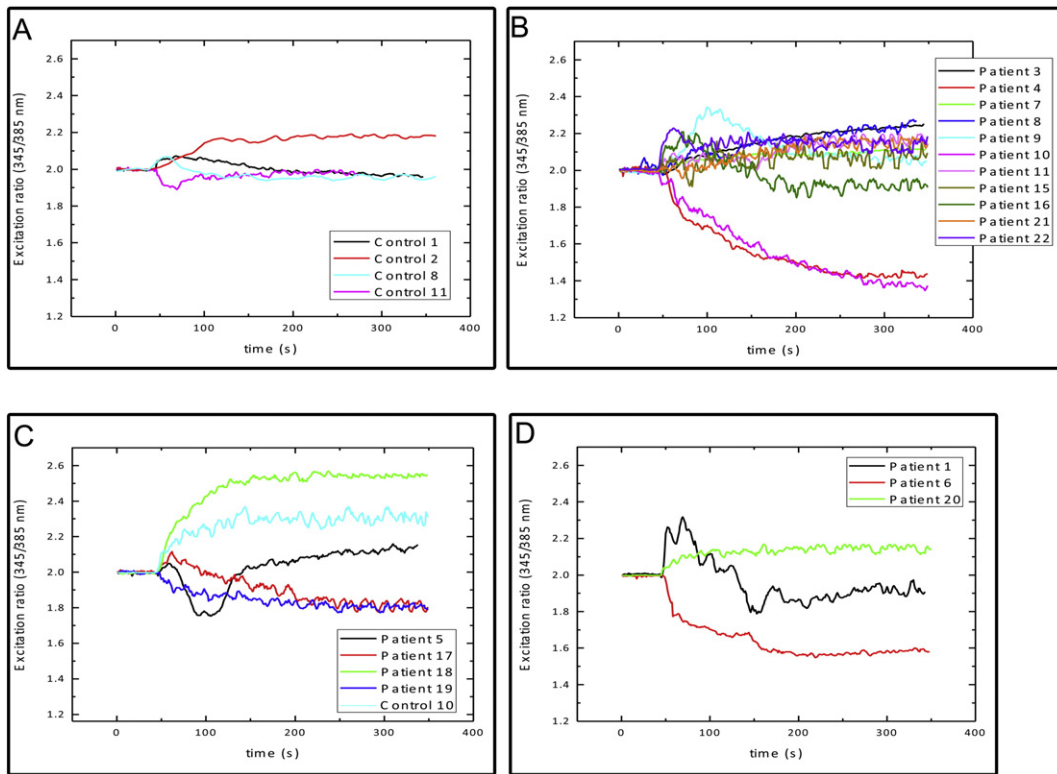

Fig. 2. Epithelial Sodium-activated Channel (ENaC) in hypertense, collagen-activated platelets. Ratios of fluorescence intensities registered at 345 and 385 nm were plotted. A) Platelet ENaC activity of representative control samples. B) Platelet ENaC activity of representative hypertensive patients' samples. C) Platelet ENaC activity shown for patients and a control belonging to the same family. D) Platelet ENaC activity shown for hypertensive patients with non-controlled blood pressure.

be quantified, we evaluated the area of resting and collagen-activated platelets from hypertensive and control subjects. We detected differences between the platelet, area although these did not show statistical significance. However, the morphological characteristics in hypertensive platelets are indicative of a hyperactivation state; this condition was corroborated with P-selectin determination by Flow Cytometry (FC) analysis (Fig. 3F). Mean Fluorescence Intensity (MFI) is significant increased for hypertensive platelets.

3.4. Hypertensive platelet membrane composition

Factors that have been shown to influence membrane fluidity include cholesterol content and fatty acid composition of the lipid bilayer; fluidity increases with decreasing cholesterol content or increasing unsaturated fatty acyl composition [22]. To confirm this assumption, we performed platelet membrane lipid composition employing the HPLC technique.
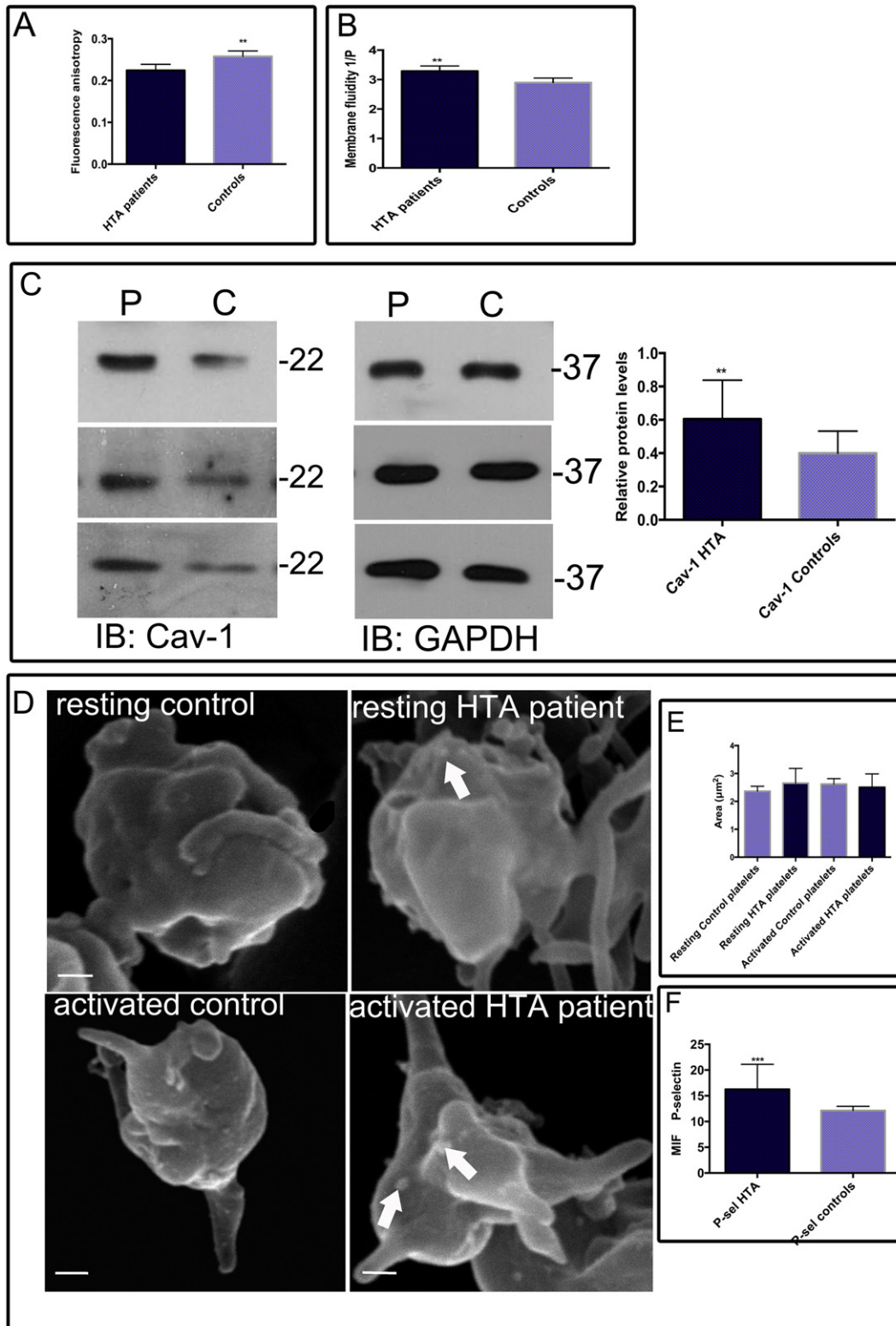
Linearity of measurement was evaluated by analyzing different concentrations (2.5×10^{-2} to 2.5×10^{-3} mg/ml) of the standards solutions. Calibration curves were constructed for combining the four standards together (Supplemental Fig. 2) and by plotting average peak area against concentration. The slope and correlation co-efficients were also determined. All of the samples were performed by duplicate.

Chromatograms of cholesterol and phospholipid standards are depicted in Fig. 4A. In the analysis of platelet lipids, individual cholesterol and phospholipid peaks were identified by comparing retention times with those of the standardized phospholipids of that particular phospholipid.

Major peaks representing retention times of 2.16, 3.00, 5.73, and 15.41 min correspond to cholesterol (1), phosphatidylserine (2), sphingosine (3), and phosphatidylcholine (4), respectively. It is noteworthy that phosphatidylcholine is a very complex molecule containing glycerol, choline, and diverse fatty acids; therefore, in the present study, we refer to the more abundant peak of this phospholipid. On the other hand, the sphingosine peak presents a displacement in patient and control samples with respect to the mixture of standards from 5.73 to 9.39 min.

Hypertensive membrane platelets had lower cholesterol and phosphatidylcholine concentrations (average range, 0.005–0.038 μg/mg protein respectively) compared with control individuals (0.01–0.095); in contrast, phosphatidylserine and sphingosine were more expressed in hypertensive subjects, with average values of 37.0 and 0.027 μg/mg of protein, respectively, compared with controls (17.4 and 0.025) (Fig. 4B).

3.5. β-dystroglycan is downexpressed in hypertensive platelets

Recently, we reported the association of β-Dystroglycan (β-Dg), an abundant transmembrane protein, with caveolin-1 in human platelets [23]; therefore, we wanted to determine the effect of caveolin-1 overexpression on β-Dg levels. To achieve this, we performed Wb of platelet lysates from hypertensive and control subjects. Bands of 43 kDa from hypertensive platelets were less intense than bands observed for control platelets, in contrast with the band observed at 50 kDa, which was more evident in hypertensive platelets (Fig. 5A). Densitometry analysis of the 43 kDa band showed that the diminution in hypertensive patients possesses statistical significance.

To confirm this downregulation, we quantified Dg mRNA by qRT-PCR assays (Fig. 5B). Our results indicate that Dg is underexpressed in hypertensive compared with normal subjects.

We also determined the expression of β-Dg PY892 in controls and hypertensive platelets. Fig. 5B shows that β-Dg PY892 bands were more expressed in lysates from hypertensive patients compared with control subjects.

It has been proposed that caveolin-1 scaffolds and organizes signalling components in proximity to receptors via a β-stranded Cav Scaffolding Domain (CSD) [24]. Because we have detected overexpressed caveolin-1, we wanted to assess the activated pattern of platelet proteins. Thus, we performed a WB assay of platelet lysates utilizing a threonine-phosphorylated antibody. Our results showed more extensive and intense threonine-phosphorylated protein pattern expression in platelets from hypertensive patients than in control platelets, suggesting a hyperactivated stage (Fig. 5C); it was corroborated with quantification of the more evident band (arrow) observed in controls and patients. The image is representative of the subjects included in the study.

3.6. β-dystroglycan is a scaffold for ENaC

Recent studies indicated that caveolin-1 is closely related with β-dystroglycan [23]. We assessed whether β-dystroglycan was essential for ENaC expression. To address this, we transfected and differentiated Meg-01 cell line to megakaryocytic lineage (platelet precursors) employing a small interfering RNA (RNAi) to target Dystroglycan (Dg RNAi). The RNAi also expressed GFP to identify unequivocally individual RNAi-treated cells. As negative control, RNAi, which is predicted not to block the translation of any specific gene, was utilized (control RNAi). Effectiveness of RNAi treatment in reducing β-dystroglycan expression in these cells was evaluated by Western blotting, immunofluorescence assays, and qRT-PCR (Supplemental Fig. 3). Through all of these methods, β-Dystroglycan reduction was evident by >50% in Green Fluorescent Protein (GFP)-expressing cells that co-express Dg-specific RNAi, compared with control RNAi-treated cells.

In order to reveal the subcellular distribution of ENaC in non-differentiated Meg-01 cells and differentiated into megakaryocytes (platelet precursors), we assayed double immunofluorescence staining utilizing an antibody raised against ENaC and TRITC-phalloidin to stain F-actin. In non-differentiated Meg-01 cells, ENaC was uniformly distributed in the plasma membrane, co-localizing with actin filaments, while in differentiated cells, ENaC was faintly observed in the cytoplasm and with a patched pattern mainly distributed in the plasma membrane that might belong to currently forming platelets. Relative ENaC levels increased during differentiation process (Fig. 6A).

To determine the impact of β-dystroglycan deficiency on ENaC, we analyzed the subcellular distribution of transfected and differentiated Meg-01 cells with confocal microscopy to detect ENaC. Images corresponding to ENaC clearly showed its overexpression, with a more intense label at the plasma membrane in RNAi-transfected cells (Fig. 6B) even more than in non-transfected differentiated cells; this observation was revealed by relative immunofluorescence units. It is important to mention that after exposure to TPA to differentiate Meg-01 cells, cytoplasmic blebs were evident and the shape of the nucleus became irregular.

We next corroborated the consequences of β-dystroglycan depletion on the relative expression level of ENaC by Western blotting. Our results demonstrated significant overexpression of ENaC in RNAi-transfected cells compared with RNAi control cells (Fig. 6C), these results confirmed by qRT-PCR assays (Fig. 6D).

4. Discussion

In the present study, we compared 25 hypertensive patients with normotensive subjects. Our results showed evidence of alterations in the biochemical and functional profile of plasma membrane platelets from hypertensive subjects.

Fig. 3. Alterations in platelet membrane fluidity, composition, and morphology in hypertensive patients. A. Platelets from hypertensive patients and controls were incubated with 1-[4-(TriMethy1Amino)-phenyl-6-Phenyl-1,3,5-Hexatriene (TMA-DPH) for 30 min at 37 °C. Incorporation of TMA-DPH intensity was measured using a spectrophotofluorometer and was registered as fluorescence anisotropy. Values shown are mean ± Standard Deviations (SD) from patients and controls. **$P < 0.05$. B. Platelets from hypertensive patients and controls were incubated with 1-[4-(TriMethy1Amino)-phenyl-6-Phenyl-1,3,5-Hexatriene (TMA-DPH) for 30 min at 37 °C. Incorporation of TMA-DPH intensity was measured using a spectrophotofluorometer and was registered as fluorescence polarization; membrane fluidity is expressed as 1/P. Values shown are mean ± Standard Deviations (SD) from patients and controls. **$P < 0.05$. C. Total lysates of hypertensive and control individuals were analyzed by Western blot utilizing antibodies against caveolin-1. Quantitative analysis using GAPDH as loading control is illustrated. Values shown are mean ± Standard deviations (SD) from bands of the 25 patients with AHT and controls. **$P < 0.005$. D. Resting and activated platelets from patients with AHT and controls were processed for scanning electron microscopy. Ultrastructure analysis of resting platelets presents some short protrusions extending from the membrane, in contrast with hypertensive platelets, which that exhibited microvesicles (white arrows) and fibrin fibers. Typical morphological changes were observed in activated platelets with the presence of long filopodia and microvesicles (white arrows), which were more evident for hypertensive platelets. Scale = 1 μm. E. Area (μm²) of control and HTA patients platelets processed for scanning electron microscopy. F. Mean Fluorescence Intensity (MFI) of P-selectin was quantified by Flow Cytometry (FC) from hypertensive patients and control individuals. Values presented are mean ± Standard Deviations (SD) from the 25 patients with AHT and controls. ***$P < 0.0005$.
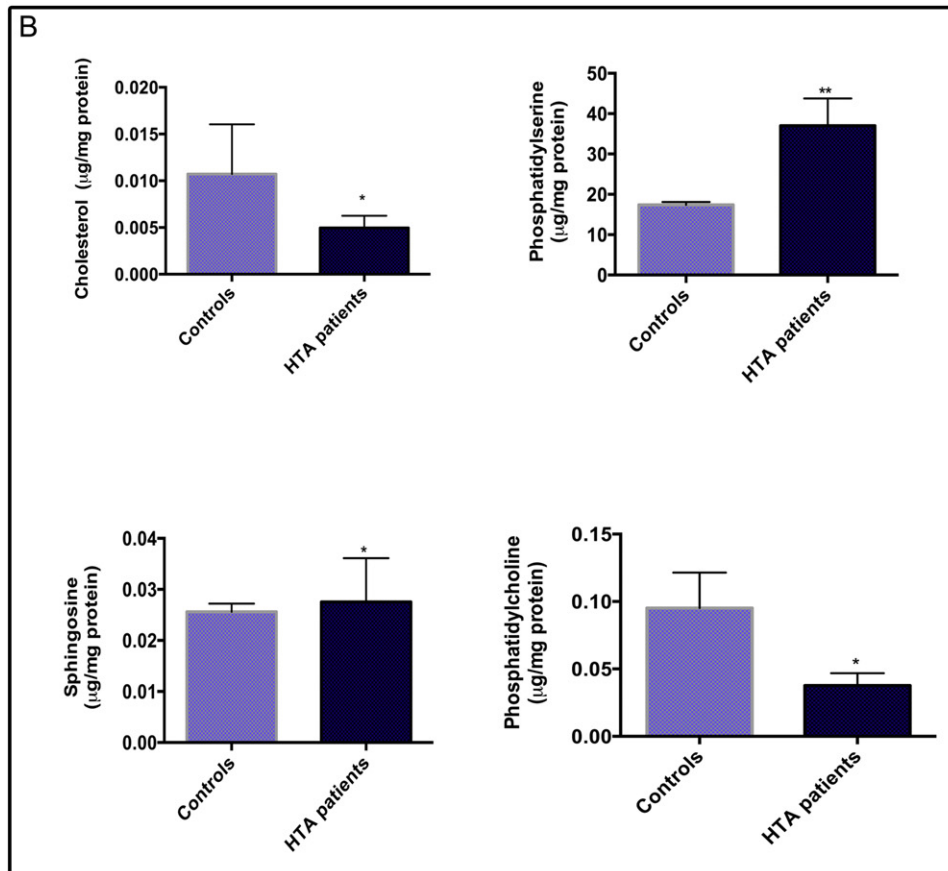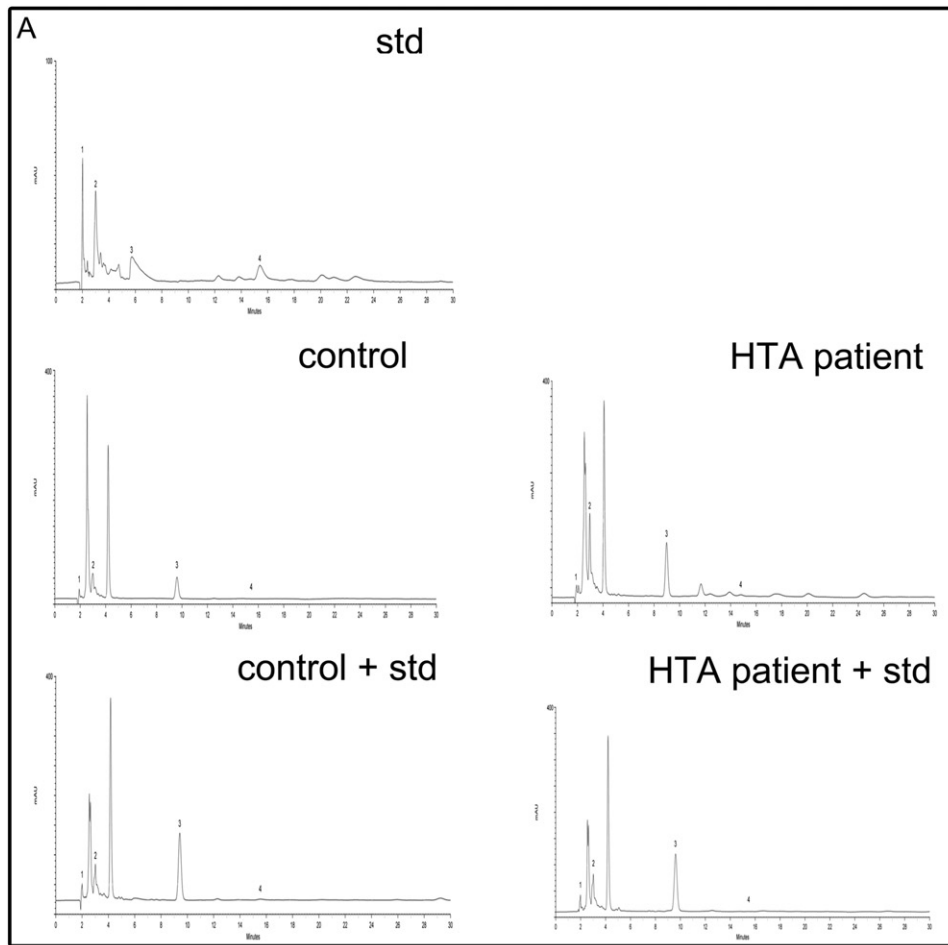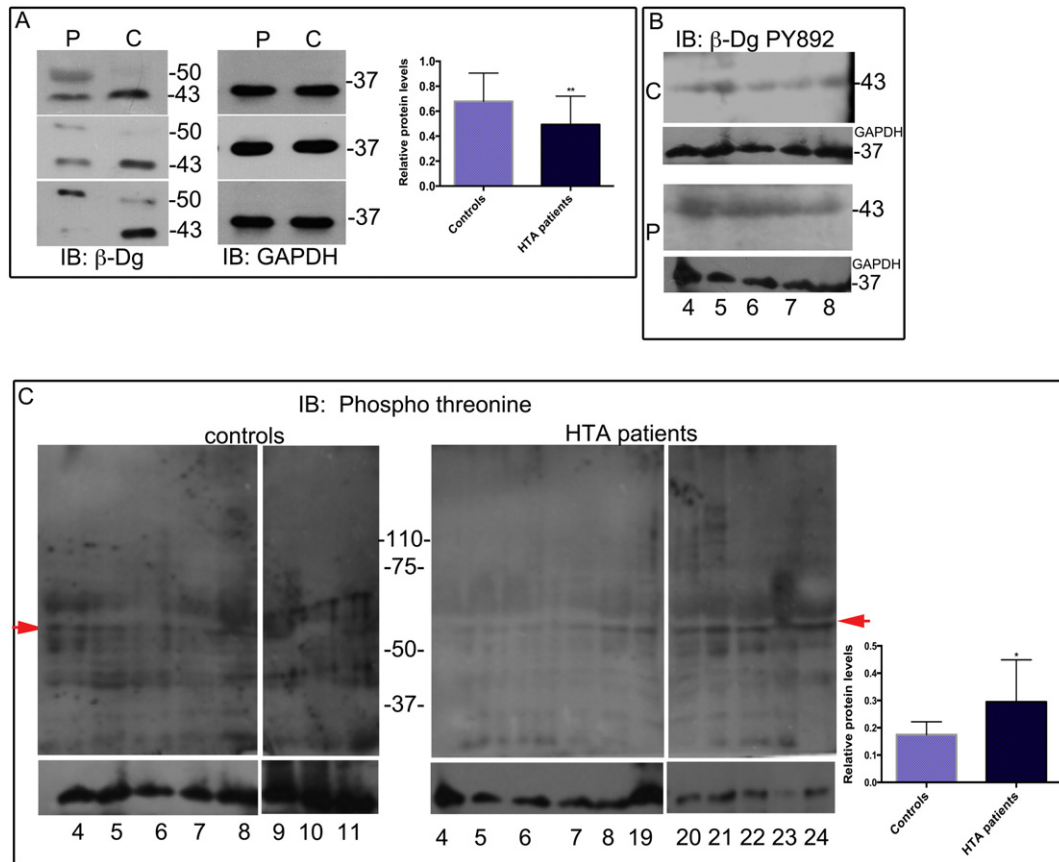
Fig. 5. β-Dg is downregulated in hypertensive patients. A. Total lysates of hypertensive and control individuals were analyzed by Western blot utilizing an antibody against β-Dg. Quantitative analyses utilizing GAPDH as loading control are depicted. Values presented are mean ± Standard Deviations (SD) from bands of 24 AHT patients and controls. **$P < 0.005$. B. Total lysates of hypertensive and control individuals were analyzed by Western blot utilizing an antibody against β-Dg PY892 (43 kDa). Representative samples of AHT patients were included. C. Total lysates of hypertensive and control individuals were analyzed by Western blot utilizing an antibody against phospho-threonine. Representative samples of AHT patients were included. Densitometry analysis of the more evident band (arrow) observed in controls and patients in Western-blot analysis. Values shown are mean ± standard deviations (SD) from three independent experiments (n = 3) *$p < 0.05$.

Arterial hypertension is associated with multiple structural and functional alterations of the cell membrane, which include changes in membrane permeability, receptor properties, signal transduction, ion transport, and calcium handling [9]; the fluidity of the lipid environment influences transmembrane proteins, modulating their transport activity characteristic of a given bilayer [25,26].

The Epithelial Sodium Channel (ENaC) mediate Na$^+$ entry into epithelial cells and play a critical role in the regulation of extracellular fluid volume and blood pressure [27]; in Liddle syndrome, deletion or truncation of ENaC subunits results in increased channel activity [28]. Recently, we described the expression of ENaC and its association pattern with cytoskeleton proteins in human platelets [12], and in the present study, we found increased expression, as well as enhanced sodium influx, in nearly all of the hypertensive individuals studied compared with controls. It has been determined that an increase in the function of ENaC in renal tissue leads to Na$^+$ retention, elevating blood pressure, which in turn depends on the increase in the number of channels expressed and on the Po state in the cell [29,30]. Increased sodium influx detected in the present study might be attributed to increased ENaC expression; however, it is feasible that in patients and controls with low sodium influx, alterations in plasma membrane could lead to conformational changes at intersubunit interfaces, which could favor the closed state of ENaC, as has been recently reported [31].

Aldosterone elevates Na$^+$ reabsorption by increasing the number (N) of ENaCs remaining at the apical membrane and directly stimulating the synthesis of the ENaC protein via an increase in production of ENaC mRNA and inhibiting its endocytosis [32,33]. This condition is worsened for obese individuals, who usually have elevated levels of circulating aldosterone [34,35].

However, Nizar et al. recently demonstrated that obesity in mice impairs natriuresis and produces elevated blood pressure that is independent of ENaC activity [36]; in addition Nesterov et al. showed that differential regulation of ENaC activity along the Aldosterone-Sensitive Distal Nephron (ASDN) does not depend on circulating aldosterone [37]. According to these evidences, we are tempted to suggest that aldosterone concentration might be exerting an influence on arterial hypertension, but not on sodium influx through ENaC nor its expression in platelets, because we did not find significant correlation among ENaC relative expression, aldosterone, and Body Mass Index (BMI) values in hypertensive patients (Supplemental Fig. 1).

Likewise, nor were BMI, aldosterone values, or blood pressure definitive for predicting sodium influx, as observed for the four hypertensive members of the same family analyzed that included a normotensive member (Fig. 2C), nor for the patients with non-controlled arterial tension (Fig. 2D). Cortisol excess may result in clinically significant hypertension; however, the plasma cortisol concentration detected in

Fig. 4. Representative ion chromatogram of AHT patients. **A.** Representative HPLC chromatograms showing standard injection (STD), control group (Control), control group in combination with standard (Control + STD), hypertensive patient (AHT patient), and hypertensive patient in combination with standard (AHT patient + STD). Major peaks correspond to cholesterol (1), phosphatidylserine (2), sphingosine (3), and phosphatidylcholine (4). **B.** Membrane platelet lipid profile in AHT patients.
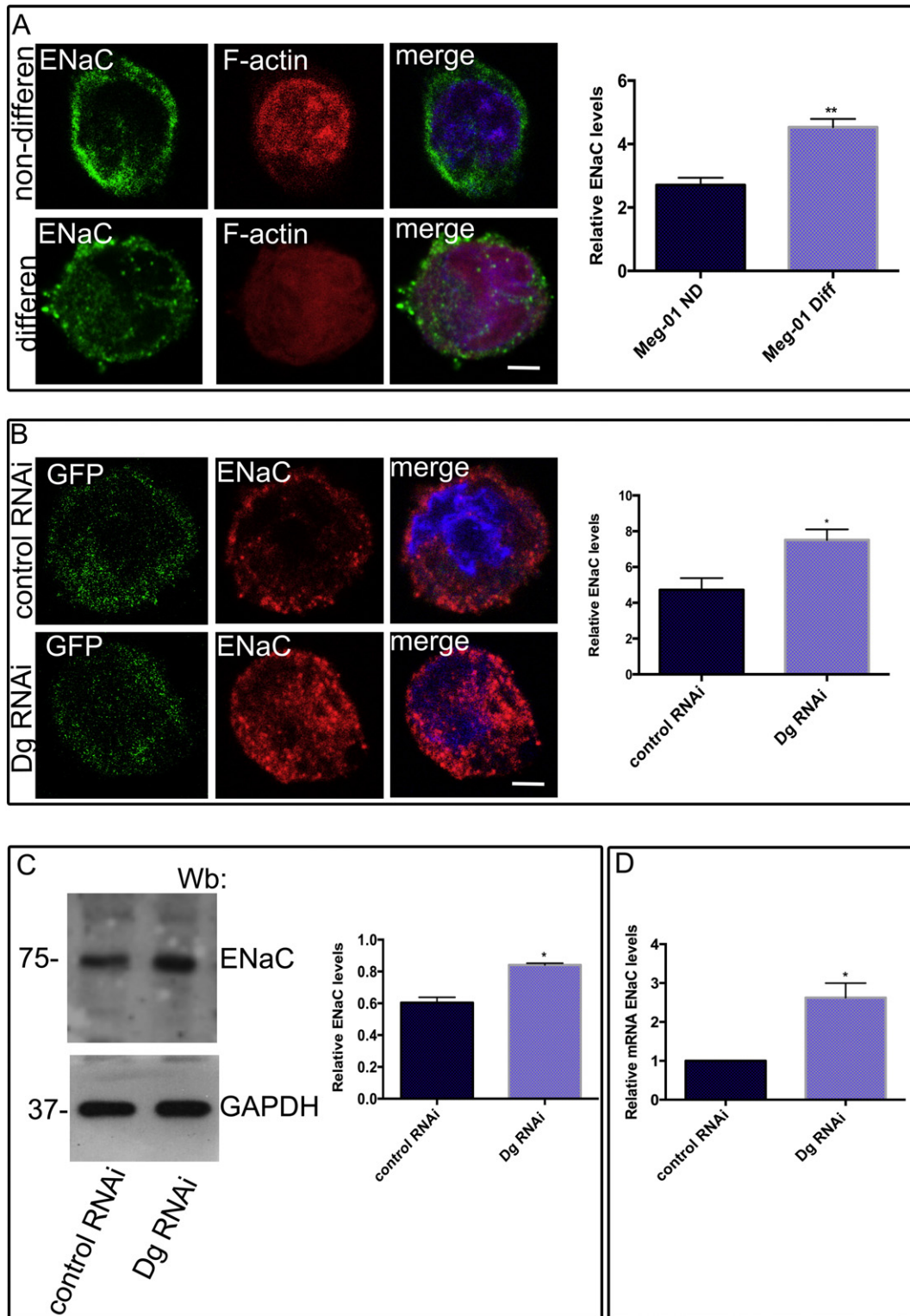
Fig. 6. β-Dystroglycan is a scaffold protein for ENaC. A. Non-differentiated and differentiated Meg-01 cells were analyzed by confocal microscopy after processing for double-labeling using antibodies directed against ENaC identified with secondary antibodies labeled with Fluorescein iso-thiocyanate (FITC) and phalloidin labeled with Tetramethyl rhodamine iso-thiocyanate (TRITC). The respective merged images are shown. Scale bar = 1.5 μm. Relative fluorescence units demonstrated significant ENaC upregulation. Values shown are mean ± Standard Deviations (SD) from three independent experiments ($n = 3$). **$P < 0.005$. B. Meg-01 cells expressing either control RNAi or Dg RNAi were immunolabeled for ENaC and analyzed for confocal microscopy. Relative fluorescence units demonstrated significant ENaC upregulation. Values shown are mean ± Standard Deviations (SD) from three independent experiments ($n = 3$). *$P < 0.005$. C. Total Meg-01 cells extracts expressing either control RNAi, or Dg RNAi were processed for Western blot, utilizing an antibody against ENaC. Densitometry analysis demonstrated ENaC overexpression in cells transfected with a Dg RNAi as compared with cells transfected with a control RNAi. Values shown are mean ± Standard deviations (SD) from three independent experiments ($n = 3$), respectively. *$P < 0.005$ D. Messenger RNA (mRNA) expression of ENaC was examined by quantitative Reverse Transcription-Polymerase Chain Reaction (qRT-PCR) in RNAi control and RNAi Dg. Values shown are mean ± Standard Deviations (SD) from three independent experiments ($n = 3$), respectively. $P < 0.05$

hypertensive and control subjects was similar, discarding the possibility that cortisol levels could contribute to high-tension values.

Membrane abnormalities in vascular smooth muscle cells, erythrocytes, lymphocytes, and platelets have been associated with intrinsic structural disturbances that are linked with hypertension, stroke, and other cardiovascular diseases [9,38].

Evidence demonstrating the presence of structural membrane abnormalities remains controversial. Several studies based on fluorescence depolarization or Spin-Label (SL) techniques indicated increased membrane microviscosity in various cells of spontaneously hypertensive rats [39,40,41,42] and of essential hypertensive patients [42].

For instance, Naftilan et al., in 1986, analyzed fluorescence depolarization with 1,6-DiPhenyl-l,3,5-Hexatriene (DPH), reporting increased microviscosity that generated a stiffer and less fluid membrane in platelets from hypertensive patients [43]. This is in contrast with the findings of Le Quan Sang et al. in 1991, who reported decreased the fluorescence anisotropy of 1-[4-(TriMethy1Amino)-Phenyl-6-phenyl-1,3,5-Hexatriene (TMA-DPH) in the platelets of hypertensive patients, indicating that hypertension was associated with increased membrane fluidity [44].

In the present study, we confirmed abnormalities in membrane platelets from hypertensive patients, evidenced by decreased fluorescence anisotropy of TMA-DPH (Fig. 3A); this indicates a lowered structural order at the external part of the plasma membrane. It is feasible that differences found with the preliminary study performed by Naftilan et al. could be attributed to the small number of patients included in the study, as well as to the use of DPH, which preferentially labels the lipid membrane core, while TMA-DPH is anchored to negatively-charged phospholipid heads at the lipid–water interface [45].

HPLC cholesterol and phospholipid quantification exhibited the plasma membrane differential composition, which in turn might disturb the asymmetry of the platelet plasma membrane [46,47,48,49], compromising its functions in hypertensive platelets [44].

Elevated blood pressure is associated with increased shear forces, especially adjacent to the endothelium, and this may lead to platelet activation and degranulation [50]. Enhanced platelet activation contributes importantly to a thrombotic state in hypertensive patients, promoting morphological and biochemical changes [6,51,52]. P-selectin expression has been considered an activation index [53], and it is known that P-selectin in circulating soluble form is increased in hypertensive patients. Moreover, platelet microparticle formation provides proinflammatory, proatherogenic, and thrombogenic properties [54]. In the present study, we confirmed platelet-activated states in hypertensive patients by quantifying P-selectin, detecting microparticles through electron microscopy and identifying the phosphorylated pattern of threonine residues from hypertensive platelets. It is feasible that platelet alterations increased platelet cytosolic Na^+ that, in turn, is exchanged for extracellular Ca^{2+}, mediating shape change, secretion, and aggregation [55], promoting constitutively activated hypertensive platelets. Phosphorylation of proteins included β-Dg, which in turn can be localized in both peripheral focal complexes and more mature focal adhesions [56], facilitating platelet adhesion, spreading and thrombus formation.

Obesity is a condition that promotes platelet activation as the result of the expanded visceral adipose depot, which is a source of cytokines and adipokines. Additionally it is also well documented that increased platelet reactivity plays a central role among the different events accelerating the risk for atherothrombosis. However, there are studies showing that, despite the fact that obese and morbidly obese subjects exhibited chronic inflammation, there was no evidence of increased platelet activation [57].

Caveolae and caveolin-1 possess a key role in orchestrating the activation of pathways that related to cell proliferation, migration, and contraction [58,59]. Cholesterol comprises a key component of caveolae and is required for proper trafficking of caveolin to the plasma membrane to other cellular sites. In platelets from hypertensive patients,

we found cholesterol diminution and overexpression of caveolin-1, which might contribute to plasma membrane instability and altered functions. Thus, membrane tension directly and indirectly might regulate ENaC-mediated Na^+ transport by affecting the Number (N) and the Probability of opening (Po) of ENaC expressed in the platelet plasma membrane.

Although we did not find correlation among ENaC, caveolin-1, and β-Dg relative expression (Supplemental Fig. 1), we suggest that β-Dg can be modulated by caveolin-1, in that we previously reported a possible interaction between caveolin-1 and β-Dg in platelet membranes [23] and in contractile myocytes [59,60]. According to the Dg downregulation results presented, we are tempted here to suggest that β-Dg is an ENaC regulatory protein acting as a structural scaffold to nucleate other regulatory elements. Our Wb analysis using the Mandag monoclonal antibody showed the expression of 50 kDa and 43 kDa bands and, although the band of 50 kDa was not revealed with the β-Dg PY892 antibody, we may suppose that it corresponds to a phosphorylated species; this is because it has reported that tyrosine phosphorylated β-dystroglycan-relative Molecular Weight (MW) depends on cell line, ranging from 43 kDa, 31 kDa, 26 kDa, 17 kDa, and 50 kDa species [61,62].

Taken together, our results show that the combination of the surrounding lipid environment and key, direct protein–protein interactions, including scaffold proteins, is required to efficiently harness and organize the wide spectrum of ENaC-regulatory components at the cell surface.

5. Conclusion

The experiments presented in this study aimed to assess the structural and biochemical differences in platelets membrane from hypertensive individuals compared to healthy individuals. Our biochemical, cell and molecular biology results demonstrated that Epithelial Sodium Channel (ENaC) is overexpressed in platelets from hypertensive patients and that characteristics and composition of platelet membrane differ from healthy individuals. Additionally, we suggest that β-dystroglycan is a scaffold protein for ENaC.

The simultaneous occurrence of membrane abnormalities described in the present study suggests that the altered dynamic properties of the cell membrane might be a common denominator of the previously mentioned changes observed in hypertension.

Better knowledge of the cellular mechanisms underlying membrane abnormalities could provide useful information concerning the development of a more specific and greater physiological approach to hypertension research.

Supplementary data to this article can be found online at http://dx.doi.org/10.1016/j.bbamem.2016.04.015.

Transparency document

The Transparency document associated with this article can be found, in online version.

References

[1] D. Varga-Szabo, I. Pleines, B. Nieswandt, Cell adhesion mechanisms in platelets, Arterioscler. Thromb. Vasc. Biol. 28 (2008) 403–412.
[2] S.S. Lim, T. Vos, A.D. Flaxman, G. Danaei, K. Shibuya, H. Adair-Rohani, M. Amann, H.R. Anderson, K.G. Andrews, M. Aryee, C. Atkinson, L.J. Bacchus, A.N. Bahalim, K.

Balakrishnan, J. Balmes, S. Barker-Collo, A. Baxter, M.L. Bell, J.D. Blore, F. Blyth, C. Bonner, G. Borges, R. Bourne, M. Boussinesq, M. Brauer, P. Brooks, N.G. Bruce, B. Brunekreef, C. Bryan-Hancock, C. Bucello, R. Buchbinder, F. Bull, R.T. Burnett, T.E. Byers, B. Calabria, J. Carapetis, E. Carnahan, Z. Chafe, F. Charlson, H. Chen, J.S. Chen, A.T. Cheng, J.C. Child, A. Cohen, K.E. Colson, B.C. Cowie, S. Darby, S. Darling, A. Davis, L. Degenhardt, F. Dentener, D.C.D. Jarlais, K. Devries, M. Dherani, E.L. Ding, E.R. Dorsey, T. Driscoll, K. Edmond, S.E. Ali, R.E. Engell, P.J. Erwin, S. Fahimi, G. Falder, F. Farzadfar, A. Ferrari, M.M. Finucane, S. Flaxman, F.G. Fowkes, G. Freedman, M.K. Freeman, E. Gakidou, S. Ghosh, E. Giovannucci, G. Gmel, K. Graham, R. Grainger, B. Grant, D. Gunnell, H.R. Gutierrez, W. Hall, H.W. Hoek, A. Hogan, H.D. Hosgood III, D. Hoy, H. Hu, B.J. Hubbell, S.J. Hutchings, S.E. Ibeanusi, G.L. Jacklyn, R. Jasrasaria, J.B. Jonas, H. Kan, J.A. Kanis, N. Kassebaum, N. Kawakami, Y.H. Khang, S. Khatibzadeh, J.P. Khoo, C. Kok, F. Laden, et al., A comparative risk assessment of burden of disease and injury attributable to 67 risk factors and risk factor clusters in 21 regions, 1990–2010: a systematic analysis for the Global Burden of Disease Study 2010, Lancet 380 (2012) 2224–2260.

[3] J.G. Diodati, R.O. Cannon 3rd, N. Hussain, A.A. Quyyumi, Inhibitory effect of nitroglycerin and sodium nitroprusside on platelet activation across the coronary circulation in stable angina pectoris, Am. J. Cardiol. 75 (1995) 443–448.

[4] S. Nityanand, B.L. Tekwani, M. Chandra, K. Shanker, B.N. Singh, Kinetics of serotonin in platelets in essential hypertension, Life Sci. 46 (1990) 367–372.

[5] P. Ferroni, F. Martini, R. D'Alessandro, A. Magnapera, V. Raparelli, A. Scarno, G. Davi, S. Basili, F. Guadagni, In vivo platelet activation is responsible for enhanced vascular endothelial growth factor levels in hypertensive patients, Clin. Chim. Acta 388 (2008) 33–37.

[6] S. Nityanand, I. Pande, V.K. Bajpai, L. Singh, M. Chandra, B.N. Singh, Platelets in essential hypertension, Thromb. Res. 72 (1993) 447–454.

[7] K.H. Le Quan-Sang, J. Levenson, A. Simon, P. Meyer, M.A. Devynck, Platelet cytosolic free Ca2+ concentration and plasma cholesterol in untreated hypertensives, J. Hypertens. Suppl. 5 (1987) S251–S254.

[8] A. Camilletti, N. Moretti, G. Giacchetti, E. Faloia, D. Martarelli, F. Mantero, L. Mazzanti, Decreased nitric oxide levels and increased calcium content in platelets of hypertensive patients, Am. J. Hypertens. 14 (2001) 382–386.

[9] J. Zicha, J. Kunes, M.A. Devynck, Abnormalities of membrane function and lipid metabolism in hypertension: a review, Am. J. Hypertens. 12 (1999) 315–331.

[10] H.A. Drummond, N.L. Jernigan, S.C. Grifoni, Sensing tension: epithelial sodium channel/acid-sensing ion channel proteins in cardiovascular homeostasis, Hypertension 51 (2008) 1265–1271.

[11] S. Kellenberger, L. Schild, Epithelial sodium channel/degenerin family of ion channels: a variety of functions for a shared structure, Physiol. Rev. 82 (2002) 735–767.

[12] D. Cerecedo, I. Martinez-Vieyra, L. Alonso-Rangel, C. Benitez-Cardoza, A. Ortega, Epithelial sodium channel modulates platelet collagen activation, Eur. J. Cell Biol. 93 (2014) 127–136.

[13] J.M. Ervasti, K.P. Campbell, Membrane organization of the dystrophin–glycoprotein complex, Cell 66 (1991) 1121–1131.

[14] O. Ibraghimov-Beskrovnaya, A. Milatovich, T. Ozcelik, B. Yang, K. Koepnick, U. Francke, K.P. Campbell, Human dystroglycan: skeletal muscle cDNA, genomic structure, origin of tissue specific isoforms and chromosomal localization, Hum. Mol. Genet. 2 (1993) 1651–1657.

[15] S. Sato, Y. Omori, K. Katoh, M. Kondo, M. Kanagawa, K. Miyata, K. Funabiki, T. Koyasu, N. Kajimura, T. Miyoshi, H. Sawai, K. Kobayashi, A. Tani, T. Toda, J. Usukura, Y. Tano, T. Fujikado, T. Furukawa, Pikachurin, a dystroglycan ligand, is essential for photoreceptor ribbon synapse formation, Nat. Neurosci. 11 (2008) 923–931.

[16] S.H. Gee, F. Montanaro, M.H. Lindenbaum, S. Carbonetto, Dystroglycan-alpha, a dystrophin-associated glycoprotein, is a functional agrin receptor, Cell 77 (1994) 675–686.

[17] M.A. Bowe, D.B. Mendis, J.R. Fallon, The small leucine-rich repeat proteoglycan biglycan binds to alpha-dystroglycan and is upregulated in dystrophic muscle, J. Cell Biol. 148 (2000) 801–810.

[18] J.M. Ervasti, K.P. Campbell, A role for the dystrophin–glycoprotein complex as a transmembrane linker between laminin and actin, J. Cell Biol. 122 (1993) 809–823.

[19] K. Russo, E. Di Stasio, G. Macchia, G. Rosa, A. Brancaccio, T.C. Petrucci, Characterization of the beta-dystroglycan-growth factor receptor 2 (Grb2) interaction, Biochem. Biophys. Res. Commun. 274 (2000) 93–98.

[20] V. Shlyonsky, A. Goolaerts, R. Van Beneden, S. Sariban-Sohraby, Differentiation of epithelial Na + channel function. An in vitro model, J. Biol. Chem. 280 (2005) 24181–24187.

[21] M. Ogura, Y. Morishima, M. Okumura, T. Hotta, S. Takamoto, R. Ohno, N. Hirabayashi, H. Nagura, H. Saito, Functional and morphological differentiation induction of a human megakaryoblastic leukemia cell line (MEG-01s) by phorbol diesters, Blood 72 (1988) 49–60.

[22] R.D. Klausner, A.M. Kleinfeld, R.L. Hoover, M.J. Karnovsky, Lipid domains in membranes. Evidence derived from structural perturbations induced by free fatty acids and lifetime heterogeneity analysis, J. Biol. Chem. 255 (1980) 1286–1295.

[23] D. Cerecedo, I. Martinez-Vieyra, D. Maldonado-Garcia, E. Hernandez-Gonzalez, S.J. Winder, Association of membrane/lipid rafts with the platelet cytoskeleton and the caveolin PY14: participation in the adhesion process, J. Cell. Biochem. 116 (2015) 2528–2540.

[24] C.L. Hoop, V.N. Sivanandam, R. Kodali, M.N. Srnec, P.C. van der Wel, Structural characterization of the caveolin scaffolding domain in association with cholesterol-rich membranes, Biochemistry 51 (2012) 90–99.

[25] P. Muriel, G. Sandoval, Nitric oxide and peroxynitrite anion modulate liver plasma membrane fluidity and Na(+)/K(+)-ATPase activity, Nitric Oxide 4 (2000) 333–342.

[26] P. Padmavathi, V.D. Reddy, P. Maturu, N. Varadacharyulu, Smoking-induced alterations in platelet membrane fluidity and Na(+)/K(+)-ATPase activity in chronic cigarette smokers, J. Atheroscler. Thromb. 17 (2010) 619–627.

[27] F.J. McDonald, P.M. Snyder, P.B. McCray Jr., M.J. Welsh, Cloning, expression, and tissue distribution of a human amiloride-sensitive Na + channel, Am. J. Phys. 266 (1994) L728–L734.

[28] R.P. Lifton, Molecular genetics of human blood pressure variation, Science 272 (1996) 676–680.

[29] L. Schild, C.M. Canessa, R.A. Shimkets, I. Gautschi, R.P. Lifton, B.C. Rossier, A mutation in the epithelial sodium channel causing Liddle disease increases channel activity in the *Xenopus laevis* oocyte expression system, Proc. Natl. Acad. Sci. U. S. A. 92 (1995) 5699–5703.

[30] J.H. Hansson, L. Schild, Y. Lu, T.A. Wilson, I. Gautschi, R. Shimkets, C. Nelson-Williams, B.C. Rossier, R.P. Lifton, A de novo missense mutation of the beta subunit of the epithelial sodium channel causes hypertension and Liddle syndrome, identifying a proline-rich segment critical for regulation of channel activity, Proc. Natl. Acad. Sci. U. S. A. 92 (1995) 11495–11499.

[31] D.M. Collier, V.R. Tomkovicz, Z.J. Peterson, C.J. Benson, P.M. Snyder, Intersubunit conformational changes mediate epithelial sodium channel gating, J. Gen. Physiol. 144 (2014) 337–348.

[32] S.Y. Chen, A. Bhargava, L. Mastroberardino, O.C. Meijer, J. Wang, P. Buse, G.L. Firestone, F. Verrey, D. Pearce, Epithelial sodium channel regulated by aldosterone-induced protein sgk, Proc. Natl. Acad. Sci. U. S. A. 96 (1999) 2514–2519.

[33] O. Staub, I. Gautschi, T. Ishikawa, K. Breitschopf, A. Ciechanover, L. Schild, D. Rotin, Regulation of stability and function of the epithelial Na + channel (ENaC) by ubiquitination, EMBO J. 16 (1997) 6325–6336.

[34] D.A. Calhoun, D. Jones, S. Textor, D.C. Goff, T.P. Murphy, R.D. Toto, A. White, W.C. Cushman, W. White, D. Sica, K. Ferdinand, T.D. Giles, B. Falkner, R.M. Carey, C. American Heart Association Professional Education, Resistant hypertension: diagnosis, evaluation, and treatment: a scientific statement from the American Heart Association Professional Education Committee of the Council for High Blood Pressure Research, Circulation 117 (2008) e510–e526.

[35] J. Scholze, E. Grimm, D. Herrmann, T. Unger, U. Kintscher, Optimal treatment of obesity-related hypertension: the Hypertension-Obesity-Sibutramine (HOS) study, Circulation 115 (2007) 1991–1998.

[36] J.M. Nizar, W. Dong, R.B. McClellan, M. Labarca, Y. Zhou, J. Wong, D.G. Goens, M. Zhao, N. Velarde, D. Bernstein, M. Pellizzon, L.M. Satlin, V. Bhalla, Sodium-sensitive elevation in blood pressure is ENaC independent in diet-induced obesity and insulin resistance, Am. J. Physiol. Ren. Physiol. (2016) (ajprenal 00265 02015).

[37] V. Nesterov, A. Dahlmann, B. Krueger, M. Bertog, J. Loffing, C. Korbmacher, Aldosterone-dependent and -independent regulation of the epithelial sodium channel (ENaC) in mouse distal nephron, Am. J. Physiol. Ren. Physiol. 303 (2012) F1289–F1299.

[38] A.F. Dominiczak, D.F. Bohr, The primacy of membrane microviscosity in genetic hypertension, Am. J. Hypertens. 4 (1991) 963–969.

[39] T. Montenay-Garestier, I. Aragon, M.A. Devynck, P. Meyer, C. Helene, Evidence for structural changes in erythrocyte membranes of spontaneously hypertension rats. A fluorescence polarization study, Biochem. Biophys. Res. Commun. 100 (1981) 660–665.

[40] M.A. Devynck, M.G. Pernollet, A.M. Nunez, I. Aragon, T. Montenay-Garestier, C. Helene, P. Meyer, Diffuse structural alterations in cell membranes of spontaneously hypertensive rats, Proc. Natl. Acad. Sci. U. S. A. 79 (1982) 5057–5060.

[41] S.N. Orlov, P.V. Gulak, I.S. Litvinov, V. Postnov Yu, Evidence of altered structure of the erythrocyte membrane in spontaneously hypertensive rats, Clin. Sci. (Lond.) 63 (1982) 43–45.

[42] I. Aragon-Birlouez, T. Montenay-Garestier, M.A. Devynck, Further analysis of cell membrane changes in genetic hypertension in rats by diphenylhexatriene fluorescence polarization, Clin. Sci. (Lond.) 66 (1984) 717–723.

[43] A.J. Naftilan, V.J. Dzau, J. Loscalzo, Preliminary observations on abnormalities of membrane structure and function in essential hypertension, Hypertension 8 (1986) II174–II179.

[44] K.H. Le Quan Sang, T. Montenay-Garestier, M.A. Devynck, Alterations of platelet membrane microviscosity in essential hypertension, Clin. Sci. (Lond.) 80 (1991) 205–211.

[45] E.M. Bevers, P.F. Verhallen, A.J. Visser, P. Comfurius, R.F. Zwaal, Bidirectional transbilayer lipid movement in human platelets as vizualized by the fluorescent membrane probe 1-[4-(trimethylammonio)phenyl]-6-phenyl-1,3,5-hexatriene, Biochemistry 29 (1990) 5132–5137.

[46] P.K. Schick, K.B. Kurica, G.K. Chacko, Location of phosphatidylethanolamine and phosphatidylserine in the human platelet plasma membrane, J. Clin. Invest. 57 (1976) 1221–1226.

[47] H.J. Chap, R.F. Zwaal, L.L. van Deenen, Action of highly purified phospholipases on blood platelets. Evidence for an asymmetric distribution of phospholipids in the surface membrane, Biochim. Biophys. Acta 467 (1977) 146–164.

[48] B. Perret, H.J. Chap, L. Douste-Blazy, Asymmetric distribution of arachidonic acid in the plasma membrane of human platelets. A determination using purified phospholipases and a rapid method for membrane isolation, Biochim. Biophys. Acta 556 (1979) 434–446.

[49] E.M. Bevers, P. Comfurius, R.F. Zwaal, Changes in membrane phospholipid distribution during platelet activation, Biochim. Biophys. Acta 736 (1983) 57–66.

[50] A. Torsellini, A. Becucci, S. Citi, F. Cozzolino, G. Guidi, V. Lombardi, D. Vercelli, M. Veloci, Effects of pressure excursions on human platelets. In vitro studies on betathromboglobulin (beta-TG) and platelet factor 4 (PF4) release and on platelet sensitivity to ADP-aggregation, Haematologica 67 (1982) 860–866.

[51] R.M. Touyz, E.L. Schiffrin, Effects of angiotensin II and endothelin-1 on platelet aggregation and cytosolic pH and free Ca2 + concentrations in essential hypertension, Hypertension 22 (1993) 853–862.

[52] J.L. Mehta, L.M. Lopez, L. Chen, O.E. Cox, Alterations in nitric oxide synthase activity, superoxide anion generation, and platelet aggregation in systemic hypertension, and effects of celiprolol, Am. J. Cardiol. 74 (1994) 901–905.

[53] G. Schmitz, G. Rothe, A. Ruf, S. Barlage, D. Tschope, K.J. Clemetson, A.H. Goodall, A.D. Michelson, A.T. Nurden, T.V. Shankey, European Working Group on Clinical Cell Analysis: Consensus protocol for the flow cytometric characterisation of platelet function, Thromb. Haemost. 79 (1998) 885–896.

[54] M. Labios, M. Martinez, F. Gabriel, V. Guiral, S. Ruiz-Aja, J. Aznar, Cytoplasmic free calcium mobilization in platelets, expression of P-selectin, phosphatidylserine, and microparticle formation, measured by whole blood flow cytometry, in hypertensive patients. Effect of doxazosin GITS, Thromb. Res. 117 (2006) 403–409.

[55] S. Heptinstall, The use of a chelating ion-exchange resin to evaluate the effects of the extracellular calcium concentration on adenosine diphosphate induced aggregation of human blood platelets, Thromb. Haemost. 36 (1976) 208–220.

[56] O. Thompson, C.J. Moore, S.A. Hussain, I. Kleino, M. Peckham, E. Hohenester, K.R. Ayscough, K. Saksela, S.J. Winder, Modulation of cell spreading and cell-substrate adhesion dynamics by dystroglycan, J. Cell Sci. 123 (2010) 118–127.

[57] G. De Pergola, N. Pannacciulli, M. Coviello, A. Scarangella, P. Di Roma, M. Caringella, M.T. Venneri, M. Quaranta, R. Giorgino, sP-selectin plasma levels in obesity: association with insulin resistance and related metabolic and prothrombotic factors, Nutr. Metab. Cardiovasc. Dis. 18 (2008) 227–232.

[58] A.W. Cohen, R. Hnasko, W. Schubert, M.P. Lisanti, Role of caveolae and caveolins in health and disease, Physiol. Rev. 84 (2004) 1341–1379.

[59] A.J. Halayko, G.L. Stelmack, The association of caveolae, actin, and the dystrophin–glycoprotein complex: a role in smooth muscle phenotype and function? Can. J. Physiol. Pharmacol. 83 (2005) 877–891.

[60] A.J. Halayko, T. Tran, R. Gosens, Phenotype and functional plasticity of airway smooth muscle: role of caveolae and caveolins, Proc. Am. Thorac. Soc. 5 (2008) 80–88.

[61] M.A. Escarcega-Tame, I. Martinez-Vieyra, L. Alonso-Rangel, B. Cisneros, S.J. Winder, D. Cerecedo, dystroglycan depletion impairs actin-dependent functions of differentiated Kasumi-1 cells, PLoS One 10 (2015), e0144078.

[62] G. Mathew, A. Mitchell, J.M. Down, L.A. Jacobs, F.C. Hamdy, C. Eaton, D.J. Rosario, S.S. Cross, S.J. Winder, Nuclear targeting of dystroglycan promotes the expression of androgen regulated transcription factors in prostate cancer, Sci. Rep. 3 (2013) 2792.